INFLUENCE OF THE LOWER HYBRID WAVE SPECTRUM ON THE CURRENT DISTRIBUTION IN ASDEX

K. McCormick, F.X. Söldner, F. Leuterer, H. Murmann, D. Eckhartt, G. Becker, H. S. Bosch, H. Brocken, A. Eberhagen, G. Fussmann, O. Gehre, J. Gernhardt, G.v.Gierke, E. Glock, O. Gruber, G. Haas, J. Hofmann, A. Izvozchikov[1], G. Janeschitz, F. Karger, M. Keilhacker[2], O. Klüber, M. Kornherr, K. Lackner, M. Lenoci, G. Lisitano, F. Mast, H. M. Mayer, D. Meisel, V. Mertens, E. R. Müller[2], H. Niedermeyer, A. Pietrzyk[3], W. Poschenrieder, H. Rapp, H. Röhr, J. Roth, F. Ryter[4], F. Schneider, C. Setzensack, G. Siller, P. Smeulders[2], K.-H. Steuer, F. Wagner, D. Zasche

Max-Planck-Institut für Plasmaphysik
EURATOM Association, D-8046 Garching

Abstract: Measurements of the plasma current density distribution j(r) during injection of stationary or propagating lower hybrid wave spectra have been performed on ASDEX. Positive current drive leads to broader j(r) profiles - while $T_e(r)$ is peaking - coupled with an increase in q from $q \lesssim 1$ to $q > 1$. The other spectra influence j(r) only to the extent predicted from classical conductivity based on changes in $T_e(r)$ under the condition $q(0) \sim 1$.

Introduction: It has been demonstrated on various experiments that lower hybrid current drive (LHCD) can be used to suppress sawtooth oscillations /1-4/ or influence m/n = 2/1 tearing modes /2-4/. Based on magnetic signals and the monitoring of MHD activity it has been conjectured that these effects have their origin in an LHCD-induced broadening of the j(r) profile /2-4/. In the same way, magnetic signals have been interpreted as inferring a strong peaking of j(r), attained by appropriately adjusting the LH wave spectrum /4/. These points have been investigated on ASDEX by direct measurements of j(r) for a variety of LH spectra.

Experiment: ASDEX was operated in the divertor configuration with parameters: $\bar{n}_e = 1.2 \times 10^{13}$ cm^{-3} ($0\pi0\pi$: 8×10^{12} cm^{-3}), I_p = 292 - 301 kA, B_T = 21.5 kG, a ~ 39.4 cm and R ~ 167 cm. Approximately 560 kW ($0\pi0\pi$: 340 kW) of rf power was launched into the plasma via an 8-waveguide grill with a phase difference $\Delta\phi$ between the waveguides such that a spectrum with $\bar{N}_\parallel \sim 2$ ($0\pi0\pi$: $\bar{N}_\parallel \sim 4$) was generated symmetrically ($0\,0\,\pi\,\pi$.., $0\,\pi\,0\,\pi$...; LHH), parallel ($\Delta\phi = +\pi/2$, LHCD) or antiparallel ($\Delta\phi = -\pi/2$) to the plasma current /5/. Z_{eff} in the ohmic heating (OH) phase - deduced assuming neoclassical conductivity - and the OH/LH loop voltages V_L are given in Table I.

The resulting incremental changes in the diamagnetic beta signal $\Delta\beta_{p\perp}$ and $\Delta(\beta_p^{equ} + l_i/2)$ (measured by poloidal flux loops) are depicted in Fig. 2. It is seen that $\Delta\beta_{p\perp}$ increases to a plateau in ~100 - 150 ms. The behavior in $\Delta(\beta_p^{eq} + l_i/2)$ is different; the initial increase in this quantity, common to all cases, is followed by a slow decrease over ~300 ms to a plateau below the OH value for $+\pi/2$ and $0\,\pi\,0\pi$. We note that $\beta_{p\perp}$ is sensitive only to the perpendicular energy $W_\perp$ and β_p^{eq} to the entire energy $W=(W_\perp+W_\parallel)/2$, so that $D = \Delta(\beta_p^{eq} + l_i/2) - \Delta\beta_{p\perp} = \Delta(W_\parallel-W_\perp)/2 + \Delta l_i/2$. Hence, the discrepancies D

[1]Academy of Sciences, Leningrad, USSR; [2]Present address: JET Joint Undertaking, England; [3]Univ. of Washington, Seattle, USA; [4]CEN Grenoble, France

seen between $\Delta\beta_{p\perp}$ and $\Delta(\beta_p^{eq} + l_i/2)$ in Fig. 2 can be ascribed to the production of a pressure anisotropy between the directions perpendicular and parallel to the magnetic field, and/or to a change in Δl_i, i.e. to a redistribution in j(r).

The effect on j(r) was determined directly by means of a neutral lithium beam probe which measures the magnetic field pitch angle $\theta_p = \tan^{-1}(B_p/B_T)$ at the intersection between the beam and optical axis of the detecting system (Fig. 1) /6-7/; j(r) can be calculated using $\theta_p(r)$ in conjunction with Maxwell's equations. $T_e(z)$ is registered along a vertical chord (not passing through the magnetic axis) by a 60 Hz pulsed Thomson scattering system (Fig. 1) /8/.

Results: The measured pitch angle profiles θ_p^c, adjusted to cylindrical geometry, for $+\pi/2$ are plotted vs. the flux-surface radius r_f in Fig. 2 (top, right) for the OH and steady-state LHCD phases along with the corresponding q(r) and j(r) profiles (top, left). It should be noted that the OH points are well documented with two points each at $r_f = -1.7$, +10.3, 14.3 and 29.2 cm. The indicated error bars on θ_p^c reflect the noise level associated with the base line of θ_p^c and of θ_p^c itself. For OH, the q=1 radius is in rough agreement with the ECE sawtooth inversion radius (hatched region) r_{st}. The application of LHCD leads to a broadening of the j(r) profile (from which $\Delta l_i \sim -0.12$ is computed) and an associated increase in q(0) from $0.98 + 0.03/-0.01$ to ~ 1.14, in concord with previous results /7/. While T_e profiles are not available for this series, the experience is always that T_e peaks with LHCD in the fashion seen with $0\ 0\ \pi\ \pi$, thereby demonstrating that the LH-driven current is decoupled from the classical conductivity profile.

The (Fig. 3) θ_p^c and T_e profiles for $-\pi/2$ exhibit no significant change between the OH and LH phases, i.e. D is due solely to a large anisotropy in the non-thermal electron population in favor of the component parallel to the magnetic field. A comparison between the experimental θ_p^c points and the curves predicted from Spitzer or neoclassical (neo) conductivity (assuming Z_{eff} and the electric field E are constant) shows no consistent agreement with either case. (Fig. 3 - the curve spread reflects the T_e error bars.) However, neither model correctly predicts r_{st}: neo gives q(0) values far below the q(0) ~ 0.96 determined from the lithium beam, whereas Spitzer generally yields q ~ 1 only very near the axis. If a central zone of anomalous resistivity or a smaller E is postulated such that q ~ 1 is fulfilled, then neoclassical conductivity would describe the experimental points reasonably well in the q > 1 region. However, for fiducial purposes the Spitzer curves are used in comparison hereafter.

The failure of the experimental θ_p^c curves to cross the axis at $r_f = 0$ for both $-\pi/2$ and $0\ 0\ \pi\ \pi$ (consecutive series) is probably due to a slight ($\sim 0.3^o$) beam misalignment. The systematic trend of the $r_f < 0$ θ_p^c points to increase for $-\pi/2$ is not understood, as a symmetric behavior for $r_f \sim 10$ cm is not observed.

The heating spectrum $0\ 0\ \pi\ \pi$ produces a pronounced peaking in $T_e(r)$, but no distinct change in θ_p^c. In contrast to the OH phase, the Spitzer θ_p^{LH} profiles lie above the experimental θ_p^c points, demonstrating that j(r) has not tracked the $T_e(r)$ change - suggestive that a mechanism which always maintains $q(0) \sim 1$ is operative.

The $0\ \pi\ 0\ \pi\ T_e^{OH}$ profile is broader in the central region compared to $0\ 0\ \pi\ \pi$, leading to a narrower j(r) distribution (synonymous with higher θ_p^c values) as corroborated by the Li-beam measurements. LHH produces a decrease in T_e ($r \leq a/2$), which j(r) follows up to $\Delta t_{LH} \sim 300 - 400$ ms as confirmed by θ_p^c from experiment (Fig. 3). Hence j(r) has been altered by affecting the bulk thermal electron population, changing $q^{OH}(0)$ from ~ 0.97 to $q^{LH}(0) \sim 1.06$ and l_i^{OH} from 1.35 to $l_i^{LH} \sim 1.15$. The behavior after $\Delta t_{LH} \sim 400$ ms cannot be considered here.

Discussion: Table I summarizes the experimentally determined changes in q(0) and l_i, from which we see that $q^{OH}(0) = 0.96 - 0.98$. This implies that only a few per cent of the current inside the q = 1 surface needs be displaced outwards in order to achieve q > 1 and an associated suppression of sawteeth. Such a small change can take place inside one sawtooth period, which is congruous with the observed invariance of r_{st} up to the moment of sawtooth disappearance described elsewhere /1/.

Taking the experimental Δl_i it is possible to compute $\Delta\beta_p^{eq}$ for all cases, the values of which are indicated on Fig. 2 by arrows. Accordingly, $+\pi/2$ produces a nearly isotropic pressure (i.e. $\Delta\beta_p^{eq} \gtrsim \Delta\beta_{p\perp}$), whereas $-\pi/2$ exhibits an extreme anisotropy and $0\ 0\ \pi\ \pi$ lies in between. These deduced trends are consistent with direct measurements of the non-thermal electron population on ASDEX /9/.

In passing it should be mentioned that the profiles discussed here are interesting candidates for a "profile consistency" analysis /10/ inasmuch as $T_e(r)$ and j(r) are loosely coupled for $0\ 0\ \pi\ \pi$ and decoupled for $\pi/2$, but both yield approximately the same T_e profile. Further, for $0\ \pi\ 0\ \pi$, LHH produces a large, coupled change in $T_e(r)$ and j(r).

Finally, the Li-beam measurements reported here support the thesis /11/ that sawtooth stabilization on ASDEX occurs only when the condition q > 1 prevails in the central region.

References:

/1/ J.E. Stevens, et al., 12th Eur. Conf. on Contr. Fusion and Plasma Physics 2, 192 (Budapest, 1985).
/2/ F. Parlange, et al., Ref. /1/, 2, 172.
/3/ D. van Houtte, et al., Nucl. Fusion Lett. 24, 1485 (1984).
/4/ D. van Houtte, et al., Course/Workshop on "Tokamak Startup-Problems and Scenarios related to the transient phases of ignited tokamak operations" (Erice, 1985).
/5/ F. Leuterer, F. X. Söldner, et al., Plas. Phys. 27, 1399 (1985).
/6/ K. McCormick, M. Kick, et al., 8th Eur. Conf. on Contr. Fusion and Plasma Physics, 140 (Prague, 1977).
/7/ K. McCormick, et al., Ref. /1/, 1, 199.
/8/ D. Meisel, H. Murmann, H. Röhr, K.-H. Steuer, this conference.
/9/ R. Bartiromo, M. Hesse, et al., this conference.
/10/ B. Coppi, Comments Plas. Phys. Contr. Fusion 5, 201 (1980).
/11/ F. X. Söldner, et al., this conference.

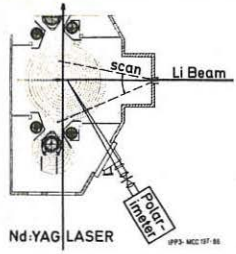

Fig. 1
Diagnostic
Layout

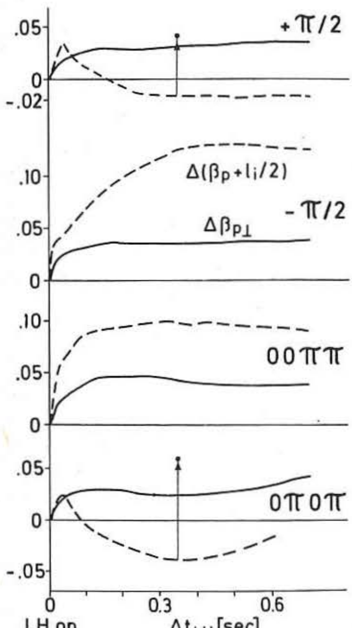

Fig. 2: The incremental change in $\beta_{p\perp}$ (-) and and $\beta_p + l_i/2$ (--) arising from LH. The arrows and points indicate the Li-beam derived values for $-\Delta l_i/2$ and $\Delta\beta_p^{eq}$, respectively. OH values: $\beta_{p\perp} \sim 0.2$, $(\beta_p + l_i/2) \sim 0.9$.

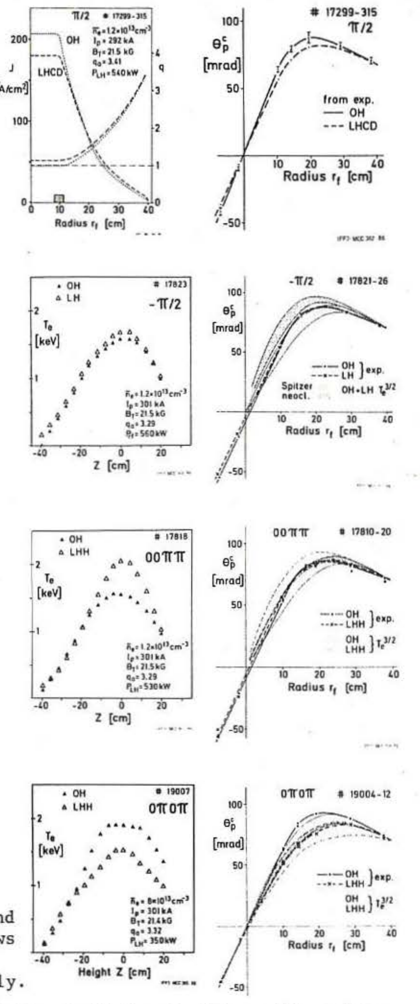

Fig. 3: j(r) and q(r) profiles (top, left) derived from the experimental pitch angle curves (top, right) for OH and LHCD. Successively, the T_e and experimental Θ_p^c profiles (on the left and right, respectively) for the OH and LH discharge phases are shown for opposite current drive $-\pi/2$, and the heating spectra, $00\pi\pi$, $0\pi0\pi$.

Table I: Experimental Results

	Z_{eff}^{neo}	$V_L^{OH}:V_L^{LH}$	$q^{OH}(0)$	$q^{LH}(0)$	Δl_i
$\pi/2$	?	0.9:0.3	0.98	1.14	-0.12
$-\pi/2$	2.4	0.9:0.62	0.96	0.99	0
$0 0 \pi \pi$	"	0.9:0.57	"	0.96	0
$0 \pi 0 \pi$	4.0	1.0:0.54	0.97	1.06(?)	-0.2